Comparing simulations of deep energy retrofits for a community centre using past and future weather scenarios

Ahmad Shoaib Amiri[1], Michael Jemtrud[2], Karine Lavigne[3], Daniel Chung[1]
[1]University of Toronto, Toronto, Canada
[2]McGill University, Montreal, Canada
[3]Hydro-Québec, Montreal, Canada

Abstract

The building sector is the largest energy-consuming sector, accounting for approximately 40% of global energy consumption, followed by industry and transport sectors. In 2050, a significant proportion of the current building stock will be in use. Therefore, the existing buildings offer a strategic opportunity to reduce energy consumption and carbon emissions (embodied and operational). This paper presents an energy modelling approach that integrates future climate scenarios into energy modelling aimed at exploring deep energy retrofits for an existing 1978 community centre located in Montreal, Quebec. This study further investigates the distribution of primary energy uses, such as heating, cooling, lighting, and ventilation and how these are influenced while examining the sensitivity of the model's energy performance to variations in climate scenarios, air infiltration rate, and the constructions of the building envelope. Further exploration will involve looking into non-mechanical means to save energy, such as adopting passive cooling design strategies, introducing temperature setbacks, and automated openings schedules. The results demonstrated an overall decrease in the heating demand, while the cooling demand tend to increase when simulating the models with future weather scenarios.

Introduction & Background

There is a growing interest in making buildings sustainable worldwide. The current energy and fuel crises, coupled with global warming and environmental problems have made architects, engineers, and building scientists rethink their approach in the design process. Buildings consume a considerable amount of energy, so their design, construction, and operation have a significant impact on fossil fuel consumption and environmental issues. The building industry is responsible for one-third of energy-related carbon emissions (Colmenar-Santos et al., 2013). A substantial portion of the building energy use occurs during the operational stage of a building (e.g., for lighting, heating, and cooling), as Bui et al. (2020) noted. Thus, it is vital to reduce energy consumption during the operational phase of a building and to ultimately reduce the impact of carbon emissions contributed by the building sector (Allouhi et al., 2015).

As a means to reduce annual energy consumption in an existing building, interdisciplinary teams of architects and engineers often work towards implementing deep energy retrofits. According to Natural Resources Canada, a deep energy retrofit (DER) involves an extensive repair of a building's systems that can save up to 60 percent of the energy costs (NRC, 2023). DER measures may include significant configurations in the interior, major repairs or adding layers to the building envelope, adding or rearranging windows for increased daylight, and often upgrading the heating, ventilation, and air-conditioning (HVAC) systems. Building energy modelling has become a significant design and decision-making tool that helps in pursuing deep energy reductions in existing residential and commercial buildings.

Global warming poses a substantial threat in terms of the energy needs and environmental problems (Ahmed et al., 2018). Therefore, a holistic process toward designing new buildings or repairing existing ones may benefit from exploring building performance under future weather conditions. Building energy modelling with future weather helps architects to not only provide design recommendations that have immediate cost and performance benefits, but also integrate predictive measures to make buildings more resilient considering global warming. The Intergovernmental Panel on Climate Change (IPCC) produced Representative Concentration Pathways (RCP) scenarios, which portray possible future greenhouse gas emission levels. This helps researchers around the world base their climate-related work around a common definition that address emission predictions through the year 2100. RCPs are defined in terms of total solar radiative forcing (W/m^2), as explained by Bass & New (2023). It is anticipated that the heating demand will decrease, while the cooling demand will increase globally (Emodi et al., 2019). Upon reviewing 93 building energy retrofit studies, Liyanage et al. (2024) pointed out that there is a significant gap in existing retrofit frameworks that simultaneously account for climate mitigation and adaptation. This is an important avenue to explore how retrofit studies can incorporate climate mitigation and adaptation strategies more effectively.

This study investigates the energy performance of Île-Bizard Community Centre (Centre socioculturel de l'Île-Bizard)—a 1978 community centre located in Montréal, Québec, under various envelope retrofits and climate scenarios to aid in retrofit design measures. As such, the sensitivity of the building energy models to alterations in various parameters including envelope constructions, air infiltration rates, weather data, and temperature setbacks are evaluated. Energy use intensity (EUI), which is a measure of annual energy use by a building divided by the building's floor area, is used as an indicator of building energy efficiency.

In this analysis, we also aim to quantify the impact of climate change on the thermal EUI of the building. It is expected that the building will go through more extreme weather events as climate change progresses. Given the anticipated impacts of climate change on building energy demands, this paper takes on a forward-looking approach, which helps designers and policymakers make informed retrofit decisions towards making buildings resilient that can withstand future climatic conditions. This study contributes to the decision-making process for energy retrofitting of municipal assets, such as community centres, by offering practical insights into improving energy efficiency of older buildings.

Methodology

Île-Bizard Community Centre has partnered with the research team and agreed to engage in a pilot DER. As part of this process, the team developed an energy model to conduct building energy simulations. The building is divided into functional spaces, including a gym, multiple offices, mechanical room, electrical room, conference rooms, and other interior spaces. The building data was collected through field study of the building, as well as by referring to the architectural drawings to construct the layout for the energy models. To explore the energy consumption of the building, two major scenarios were selected: (1) pre-retrofit, and (2) post-retrofit. The aim was to explore the variations and sensitivity in the annual energy consumption under present and future climate conditions along with a range of air infiltration rates.

Building location

The IB Community Centre (Figure 1) is located in Île Bizard, near Montreal. In this study, we modelled the building's energy performance under a baseline case (i.e. existing and referred to as "pre-retrofit case" in the article), as well as retrofit scenario constructions. The summary of inputs related to the building and its location is provided in Table 1. For this building, the ASHRAE climate zone was set to 6A in the Site Location inputs as per the *ANSI/ASHRAE 169-2020 (Climate Data for Building Standards)*.

Figure 1: Photograph of the building

Table 1: Building and site information

Parameter	Value
Building location	Latitude: 45.43 Longitude: -73.93
Elevation from sea level	39 m
Building orientation	45° relative to the North
Roof type	Gable roof
Roof angle	9°
Number of floors	2
Floor area	1250.12 m^2
Wall height	5.9 m
Total building height	7.6 m
Construction year	1978

Weather files

Building energy modelling uses the nearest meteorological weather data to a location of interest. As a fixed geographical location to obtain weather data, Montréal-Pierre Elliott Trudeau International Airport (station number: 716270), having a distance of 10.95 km from the IB Community Centre, was selected. In this research,

In this research, we used four variations that fall under the following three categories:

1. An actual meteorological year (AMY), which represents the actual hourly weather data sets that have been collected for a specific location, for a specific year. The year 2021 AMY was selected for this research.
2. A typical meteorological year (TMY) is statistically collected by months from multi-year time periods for a given geographical location to represent a typical year without extremes. In this project, a TMY weather file derived from 2007 - 2021 was selected.
3. Future weather years in the project were based on Representative Concentration Pathway (RCP) models by the IPCC to quantify future greenhouse gas concentrations, as well as weather files generated using the Climate Change Weather File Generator (CCWeatherGen). In this paper, CCWeatherGen is denoted by CCWG. Out of the four RCP pathway scenarios (i.e., RCP 2.5, RCP 4.5, RCP 6.0, and RCP 8.5) two pathways selected for this research are RCP 4.5 (moderate emission) and RCP 8.5 (high emission). According to Jentsch et al. (2013), CCWG weather files represent 'medium–high' emission scenario. For both

RCP pathway scenarios and generated CCWG weather data 2050 and 2080 were used.

The 2021 AMY was obtained from SIMEB (Simulation énergétique des bâtiments) weather data. The TMY is from Climate One Building database. The RCP 8.5 weather files were derived from The Pacific Climate Impacts Consortium (PCIC). The RCP 4.5 weather files were obtained from Meteonorm global climate database.

Thermal resistance

Thermal resistance, the reciprocal of the heat transfer coefficient (*U*-factor) is often referred to as RSI or R-value. RSI is represented in units of m^2·K/W (R-value in h·ft^2·°F/BTU). As part of this research, we investigated the RSI of the building envelope at IB. THERM 7.8, developed by Lawrence Berkeley National Laboratory (LBNL), was used to model the RSI of the base- and retrofit-case enclosures. There are two types of wall sections that were used in the construction of the original wall assembly for IB: (1) A 177mm thick wall section, that was used on a portion of the South and the North sides; and (2) a 330mm thick wall that is the wall section used for all other parts of the building, each section covering 18.5% and 81.5% of the total wall area, respectively. Figure 2 shows the base-case and retrofit-case scenarios with the 330mm original wall sections in THERM. For the 177mm section, the retrofit portion is the same as shown in Figure 2. However, the original portion differs as it does not include the 4-1/2" unventilated air cavity, and the fiberglass insulation is 4" thick. The thermal properties of the materials are based on the commercial product specifications, as well as the standard values from *2021 ASHRAE Handbook (Fundamentals)*. For the interior side, the surface film resistance is 0.12 m^2·K/W (0.68 h·ft^2·°F/BTU). For exterior side (winter conditions), the surface film resistance is 0.030 m^2·K/W (0.17 h·ft^2·°F/BTU). The temperature difference between the surfaces was assumed to be 21 °C (70 °F) per Chapter 26th of the *2021 ASHRAE Handbook (Fundamentals)*.

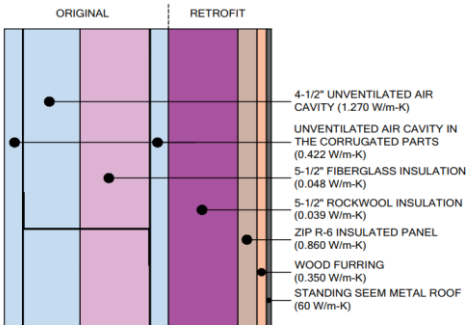

Figure 2: 330mm wall: original (base) and retrofit-case

RSI in-situ measurements

To determine the actual RSI of the wall assembly, a mock-up of the original wall assembly was constructed at the Centre for Advanced Building Envelope Research (CABER)— at Carleton University. This wall assembly was built based on the original 330mm wall section of the IB building, for which the RSI was measured to be 1.526 m^2·K/W (8.665 h·ft^2·°F/BTU). In addition, infrared thermography (IRT) was used to determine the spatially averaged U-factor of the envelope. In this procedure, as proposed by Chung (2015), we use data collected using heat-flux and temperature sensors to calculate the heat transfer coefficients for the air films and spot locations, and to eventually derive the spatial average of the U-factor for a larger section of the envelope. As such, an IRT photos were recorded using a FLIR *T540SC* having an infrared resolution of 464 × 348 pixels. This was used to collect surface temperature data to calculate U-factor values of the assembly, in conjunction with the in-situ heat-flux and temperature measurements using sensors that were installed at the building (shown in Figure 3A): (1) North side weather station, installed on a 330mm wall section; and (2) South side weather station, installed on a 177mm wall section, from which heat-flux (Q_i), indoor (T_{in}) and outdoor temperature (T_{out}) data were collected. The temperature measured using a third station installed at the West side of the building was also taken into account in the calculations. *ASTM C1155-95 Standard Practice for Determining Thermal Resistance of Building Envelope Components from the In-Situ Data* provides guidelines on determining RSI of an envelope using the in-situ weather data measurements.

Using the thermal images collected, we then determined indoor surface temperature (T_{is}) and outdoor surface temperature (T_{os}). Using this data, we then derived the empirical resistance of the air film using the following equations, as proposed by Chung (2015):

$$R_{ai} = |T_{in} - T_{is}|/Q_i \quad (2)$$

$$R_{ao} = |T_{os} - T_{out}|/Q_i \quad (3)$$

where R_{ai} and R_{ao} are the resistance of inside and outside air films, respectively, in m^2·K/W. The resistance of the envelope, R_{env}, is then determined using the following equation:

$$R_{env} = \frac{R_{ao}\,(|T_{in} - T_{os}|)}{|T_{os} - T_{out}|} - R_{ai} \quad (4)$$

When using inside surface temperatures, the above equation transforms to Equation 5.

$$R_{env} = \frac{R_{ai}\,(|T_{is} - T_{out}|)}{|T_{in} - T_{is}|} - R_{ao} \quad (5)$$

Infiltration Rate in-situ measurement

Modelling infiltration is a crucial aspect of building performance energy simulation. In order to get a better understanding of the current infiltration rate at the IB Community Centre and to be able to use a measured value within the base-case energy model, an in-situ blower door test was carried out. The equipment used in this test was a *Model 3 (110V) Blower Door Fan* manufactured by *The Energy Conservatory*. The test mode was depressurization. The results showed an infiltration rate of 3.27 air changes per hour (ACH) at an induced pressure of 50 Pa. ACH50

indicates the number of times per hour the entire volume of air in the building is replaced when the building enclosure is subjected to a pressure of 50 Pa. The blower door results were reported as 11570 cubic feet per minute. Ismaiel et al. (2023) reports that the airtightness across the Canadian buildings range between 2.8 to 4.4 ACH50. Khemet & Richman (2020) studied the ACH50 measurements across 900,000 single-family homes in Canada and presented a mean of 5.7 ACH50. In this research, an input of 3.27 ACH50 is then used in the base-case energy model using DesignBuilder software. Figure 3B shows the in-situ blower door measurement at IB Community Centre. The corresponding air infiltration rate in the units of air changes per hour natural simulated in the model is 0.21 hr^{-1}.

Three air infiltration rates were selected to be used in the models. This helps in investigating the impact of various air-tightness levels under each scenario. The infiltration rates are: (1) ACH50 = 0.6 (exceptional airtightness); (2) ACH50 = 3.27 (moderate airtightness); (3) ACH50 = 7.5 (poor airtightness).

Figure 3A (left): Sensors at the IB Community Centre; Figure 3B (right): In-situ blower door measurement

Actual building energy consumption

To model past building energy consumption and establish a baseline model (i.e., the pre-retrofit case), we used past metered data. IB building management agreed to share smart metered data from 2021 to establish a baseline model. The energy end uses are divided into three categories: (1) heating; (2) cooling; and (3) base load, where the base load accounts for equipment and plug loads. While heating loads dominate in many buildings in Canada, the IB Community Centre is a unique case since the building also feeds circuits used for outdoor events. IB is an all-electric building, and the heating is done with resistance heating. This building powers several parking lights, and a pool house located in the same complex. Building's energy reports list 2021 annual EUI of 311.91 kWh/m^2. A regression analysis of the hourly consumption against the outside air dry bulb temperature was conducted, which breaks down the total EUI into three parts: Base EUI = 175.26 kWh/m^2, Heating EUI = 101.54 kWh/m^2, and Cooling EUI = 35.12 kWh/m^2. Base EUI includes any non-thermal energy consumption (heating and cooling). Given the available insights on the actual energy consumption for 2021, the year *2021* was selected for validation of the baseline model.

Building energy performance simulation

A 3D model of the building is shown in Figure 4. Construction layers, for walls and the roof, were added as based on assumptions for the building's existing and retrofit scenarios. The simulations are carried out using the basic EnergyPlus *ZoneHVAC:IdealLoadsAirSystem* method, in which the heating and cooling load calculations are based on the heat flows.

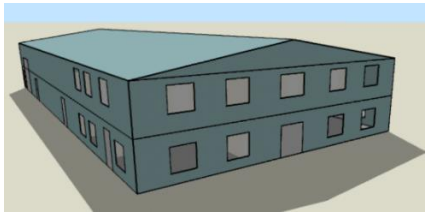

Figure 4: DesignBuilder model for IB Community Centre

The lighting power densities and plug loads are estimated using ASHRAE Standard 90.1. The inputs used in DesignBuilder model are listed in Table 2.

Table 2: Inputs used in DesignBuilder

Parameter	Location	Value
Occupancy density (people/m^2) Based on survey of the building)	Gym	0.12
	Daycare	0.16
	Offices	0.41
	Knitting club	0.13
	Other rooms	0.21
Lighting power density (W/m^2)	Electrical room	16
	Offices	24.22
	Gym	13.89
	Mechanical Room	16
	Daycare	21.10
	Conference Rooms	26.80
	All other spaces	15
Mechanically ventilated fresh air by ASHRAE Standard 62.I (2022) requirements (L/s.person) (These are for the model with fresh air inputs)	Classrooms	5
	Gym	10
	Kitchen	3.8
	Other rooms	2.5
Equipment power density (W/m2)	Gym	1
	Conference Rooms	1
	Offices	10.8
	Daycare	5
Heating set point temperature	Whole building	21.5 °C
Cooling set point temperature	Whole building	23.0 °C
Infiltration rate	Whole building	3.27 ACH50

Other non-geometrical properties of the building, including temperature setpoints and occupancy schedules were obtained through a building survey and interview with the building manager to input in the models. The heating temperature setpoint is 21.5 °C and the cooling temperature setpoint is 23 °C.

For the pre-retrofit cases a constant interior setpoint was used. To further explore the sensitivity of the model to temperature setbacks, this parameter was introduced for post-retrofit scenarios. *ANSI/ASHRAE/IES 90.1-2022 - Energy Standard for Sites and Buildings Except Low-Rise Residential Buildings* recommends an adjustable heating setpoint at least 5.6 °C below the heating setpoint, and an adjustable cooling setpoint at least 2.8 °C above the cooling setpoint. Thus, in this project, we used heating and cooling temperature setbacks of 15.9 °C and 25.8 °C, respectively, for the retrofit models designated with "WTS" (With Temperature Setback).

The weather files were imported for each scenario to run the simulations as per climate conditions under each scenario. Figures 5 shows the modelling scenarios under pre- and post-retrofit cases, where:

- FTS = fixed temperature setpoint
- WTS = with temperature setback
- EUI = energy use intensity
- ACH50 = air changes per hour at 50 Pa

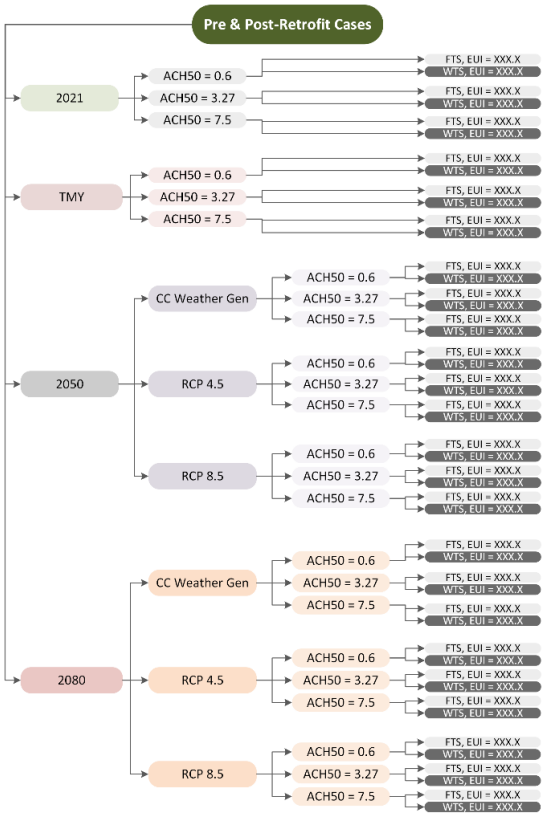

Figure 5: Pre- and post-retrofit scenarios

Results and discussion

This section presents the results of the RSI modelling and in-situ calculations, as well as the annual energy consumption results based on the pre- and post-retrofit scenarios outlined in methodology.

RSI results: THERM modelling and in-situ measurements

Figure 6 shows the THERM values for the 330 mm wall pre-retrofit case, along with the colour flux vectors and magnitude, representing the temperature variation across the assembly and the effect of thermal bridging. It is evident that there is some thermal bridging that occurs due to the z-girts. Table 3 summarises the results of the THERM models for both wall sections.

Table 3: RSIs from THERM modelling

Wall assembly		Resistance in m^2·K/W (h·ft2·°F/BTU)
177mm section	Pre-retrofit	1.234 (7.00)
	Post-retrofit	4.954 (28.13)
330mm section	Pre-retrofit	1.612 (9.15)
	Post-retrofit	5.35 (30.35)

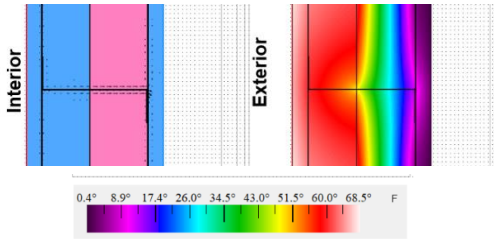

Figure 6: 330mm wall section in THERM

The RSIs of the larger sections of the wall assembly were determined using the thermal images, as well as in-situ sensors. Figure 7 shows a thermal image and a photograph of the South wall of the IB Community Centre.

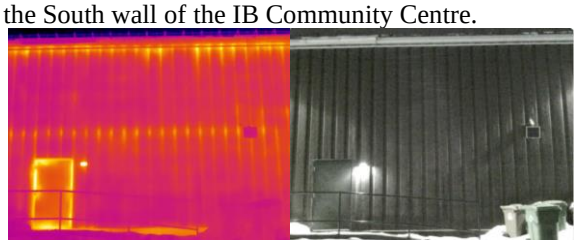

Figure 7: Thermal image and the photograph of the South wall

With thermal images captured from all sides of the wall assembly on the exterior, in conjunction with thermal images from the indoor wall surfaces, spot-measurements were carried out for portions of the wall assembly. Based on the in-situ heat-flux data collected by the sensors, the mean of the measured heat-flux values for 177mm and 330mm walls are calculated to be 8.386 W/m^2 and 14.738 W/m^2, respectively. Table 4 indicates the in-situ values for a portion of the North wall (330mm section).

Table 4: In-situ values of a portion of the North wall

Calculated average Q_i	Measured average T_{out}	Measured average T_{os}	Calculated average Resistance
14.738 W/m^2	0.39 °C	0.4 °C	2.433 m^2·K/W
4.672 BTUK/h·ft^2	32.70 °F	32.72 °F	13.82 h·ft^2·°F/BTU

After carrying out the spot-measurements for each thermal image and analyzing the results, spatial average RSI were calculated both for the 177mm and 330mm wall sections, while accounting for the area distribution among the entire wall assembly. The mean RSIs are shown in Table 5.

Table 5: Spatial average R-RSIs for the wall assembly

Mean thermal resistance of 177mm walls	Mean thermal resistance of 330mm walls
1.300 m^2·K/W	2.352 m^2·K/W
7.382 h·ft^2·°F/BTU	13.356 h·ft^2·°F/BTU

For the DesignBuilder model, the RSIs from the mean spatial averages for 177mm and 330mm walls (indicated in Table 5) are used for the pre-retrofit cases. For post-retrofit cases, however, since the panels are not built, and as a result, no in-situ measurements are available, we used the RSIs calculated from the THERM post-retrofit models, mentioned in Table 3, for the wall assembly.

For the roof, the calculated thermal resistance of the pre- and the post-retrofit cases used in energy models are 2.821 m2·K/W (16.019 h·ft^2·°F/BTU) and 13.234 m2·K/W (75.150 h·ft^2·°F/BTU), which are based on the original and proposed assemblies.

Building energy simulation results: pre- and post-retrofit scenarios

Figures 8A, 8B & 8C summarise the results of the pre- and post-retrofit scenarios in terms of energy use intensity (kWh/m^2). Comparing the models with the same constructions, we can see the models with AMY resulted in higher EUI compared to TMY weather data in all models. The EUI gradually increases with the models that use future weather data from moderate to more aggressive scenarios. A similar trend is followed by the cooling demand as we can observed higher cooling needs with RCP 4.5, RCP 8.5, and CCWG.

The temperature setbacks further led to a decrease in the thermal EUI across all weather scenarios, which proves to be one of the effective means in saving energy.

To get a better understanding of the model's sensitivity to variations in climatic data, Figures 9 & 10 compare various past and future climatic scenarios across the models having 3.27 ACH50 with pre-retrofit constructions. As we can see from Figure 9, the TMY model has a lower EUI compared to other scenarios. In contrast, an AMY weather file represents more realistic climatic condition of a location compared to TMY weather data. Often, the TMY weather files omit extreme weather days since they are derived statistically over a long period of time and such files account for average conditions.

Figure 9 shows that the heating EUI seems to fall in the same range across all scenarios, except the TMY model. However, looking at the cooling EUI, it is evident that the cooling EUI increases when we move toward more aggressive future climate scenario projects, as we can see an increase in the cooling and the overall EUI from RCP 4.5 to RCP 8.5. CCWG-based models behave similar to RCP 8.5. However, CCWG weather scenario seems to have the highest impact on the cooling EUI among other future scenarios. This could be due to higher temperatures during the summer and/or a higher frequency in hot days.

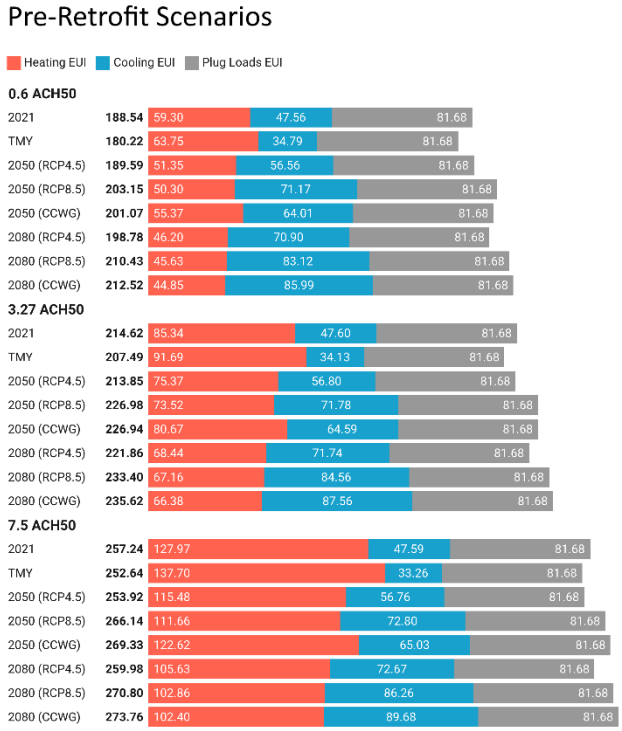

Figure 8A: Pre-retrofit results in kWh/m^2

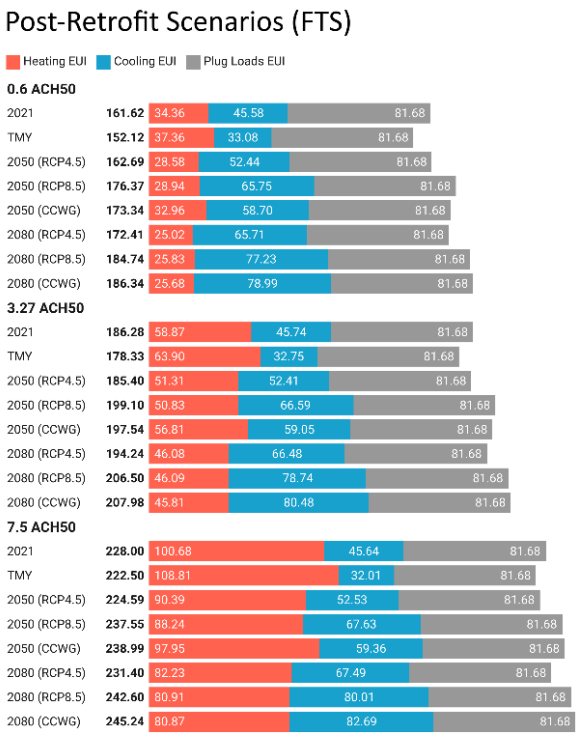

Figure 8B: Post-retrofit (FTS) results in kWh/m^2

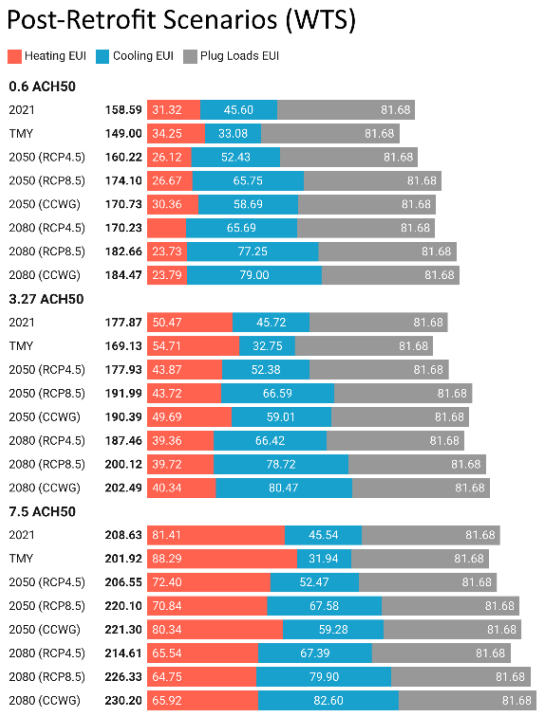

Figure 8C: Post-retrofit (WTS) results in kWh/m²

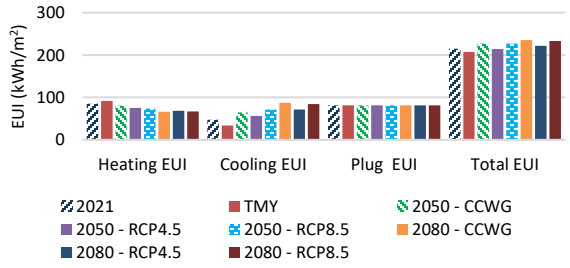

Figure 9: EUI of 3.27 ACH50 pre-retrofit models across various climate scenarios

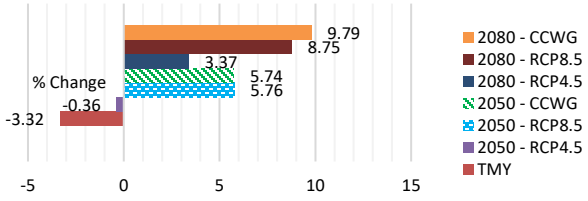

Figure 10: Percent change of the 3.27 ACH50 pre-retrofit models across various climate scenarios

Further comparing the 2021 models having the same infiltration rate (i.e., 3.27 ACH50) with varying RSI and constructions in Figure 11, we can observe a percent decrease of 13.20% between the pre-retrofit and the post-retrofit (FTS) and a percent decrease of 17.12% between the pre-retrofit and post-retrofit (WTS) models. When comparing the pre-retrofit models having the 2021 weather file and same constructions while varying the infiltration rates yields a percent increase of 13.84% in overall EUI from the 0.6 ACH50 to the 3.27 ACH50 and changing the infiltration rate from 0.6 ACH50 to 7.5 ACH50 results in a percent increase equal to 36.44%.

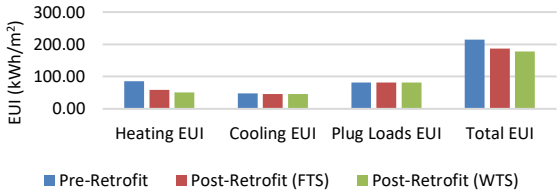

Figure 11: Pre- and post-retrofit models having 2021 AMY weather data

All the models account for the minimum fresh air requirements recommended by ASHRAE Handbook of Fundamentals. This results in an increase in the overall thermal EUI of the building in both the pre- and post-retrofit cases. To further assess the impact of mechanically ventilated fresh air beyond the above reported results, the minimum fresh air inputs were set to zero in the pre-retrofit and the post-retrofit (FTS) models having 3.27 ACH50 with 2021 AMY weather data. For the pre-retrofit case with no mechanically ventilated fresh air, the overall EUI was simulated to be 169.47 kWh/m2, resulting in a percentage decrease of 21.04%. The simulated EUI of the post-retrofit (NTS) model with minimum fresh air inputs set to zero was 143.94 kWh/m2, which resulted in an overall EUI saving of 22.73% when compared to the post-retrofit (NTS) model with minimum fresh air inputs.

Conclusion

A sensitivity analysis of the building energy model reveals that, while we can expect reductions in heating demands with raising global temperatures, we might encounter higher cooling energy. Another important area that requires further work is developing a holistic approach in modelling RSIs in light of climate change. Although RSI provides a significant insight into an envelope's current performance, there is a need to investigate the potential degradation of RSI with time. Finally, developing and adopting passive techniques to save energy can play a significant role in reducing the energy demand, such as utilizing smart thermostats that can adopt to occupants' behaviour and activates temperature setbacks when needed. At the time of publishing this paper, the retrofits were not conducted yet. Additionally, the submetering data was not available, and hence, the model is not fully validated yet. Future research will further juxtapose the simulated and the actual impact of retrofits. The resiliency of the building (i.e., building's liveability in case of extreme weather events and power outage) will be investigated in future work.

Acknowledgement

This research is supported by the research funding provided by the Natural Sciences and Engineering Research Council

of Canada (NSERC) of Canada, Hydro-Québec and Quebec Ministry of Energy and Natural Resources, Energy Transition sector.

References

Ahmed, N., Khan, T. I., & Augustine, A. (2018). CLIMATE CHANGE AND ENVIRONMENTAL DEGRADATION: A SERIOUS THREAT TO GLOBAL SECURITY. European Journal of Social Sciences Studies, 0, Article 0. https://doi.org/10.46827/ejsss.v0i0.394

Allouhi, A., El Fouih, Y., Kousksou, T., Jamil, A., Zeraouli, Y., & Mourad, Y. (2015). Energy consumption and efficiency in buildings: Current status and future trends. Journal of Cleaner Production, 109, 118–130. https://doi.org/10.1016/j.jclepro.2015.05.139

American Society of Heating, Refrigerating and Air-Conditioning Engineers. (2021). ASHRAE Handbook—Fundamentals. Retrieved March 29, 2024, from https://www.ashrae.org/technical-resources/ashrae-handbook/description-2021-ashrae-handbook-fundamentals

American Society of Heating, Refrigerating and Air-Conditioning Engineers. (2022). ANSI/ASHRAE Standard 62.1-2022: Ventilation for Acceptable Indoor Air Quality. Atlanta, GA: ASHRAE. Retrieved from https://www.ashrae.org/technical-resources/bookstore/standards-62-1-62-2#:~:text=ANSI%2FASHRAE%20Standard%2062.1%2D2022,that%20minimizes%20adverse%20health%20effects.

American Society of Heating, Refrigerating and Air-Conditioning Engineers. (2020). ASHRAE Standard 169-2020: Climatic Data for Building Design Standards. Atlanta, GA: ASHRAE.

ANSI/ASHRAE/IES 90.1. (2022). Energy Standard for Sites and Buildings Except Low-Rise Residential Buildings. Retrieved March 14, 2024, from https://webstore.ansi.org/standards/ashrae/ansiashraeies902022.

American Society for Testing and Materials. (2021). Standard Practice for Determining Thermal Resistance of Building Envelope Components from the In-Situ Data. ASTM International.

Bass, B., & New, J. (2023). How will United States commercial building energy use be impacted by IPCC climate scenarios? Energy, 263, 125945. https://doi.org/10.1016/J.ENERGY.2022.125945

Bui, D. K., Nguyen, T. N., Ghazlan, A., Ngo, N. T., & Ngo, T. D. (2020). Enhancing building energy efficiency by adaptive façade: A computational optimization approach. Applied Energy, 265, 114797. https://doi.org/10.1016/J.APENERGY.2020.114797

Colmenar-Santos, A., Terán De Lober, L. N., Borge-Diez, D., & Castro-Gil, M. (2013). Solutions to reduce energy consumption in the management of large buildings. Energy and Buildings, 56, 66–77. https://doi.org/10.1016/J.ENBUILD.2012.10.004

Chung, D. (2015). Historic Building Facades: Simulation, Testing and Verification for Improved Energy Modeling. Journal of the National Institute of Building Sciences, Vol. 3, No.1, 16-21.

Emodi, N. V., Chaiechi, T., & Alam Beg, A. B. M. R. (2019). A techno-economic and environmental assessment of long-term energy policies and climate variability impact on the energy system. Energy Policy, 128, 329–346. https://doi.org/10.1016/j.enpol.2019.01.011

Ismaiel, M., Gouda, M., Li, Y., & Chen, Y. (2023). Airtightness evaluation of Canadian dwellings and influencing factors based on measured data and predictive models. Indoor and Built Environment, 32(3), 553-573.

Jentsch, M. F., James, P. A., Bourikas, L., & Bahaj, A. S. (2013). Transforming existing weather data for worldwide locations to enable energy and building performance simulation under future climates. Renewable energy, 55, 514-524.

Khemet, B., & Richman, R. (2020). Towards a methodological approach to builder specific, preconstruction airtightness estimates for light-framed, detached, low-rise residential buildings in Canada. Journal of Building Engineering, 29, 101140.

Liyanage, D. R., Hewage, K., Hussain, S. A., Razi, F., & Sadiq, R. (2024). Climate adaptation of existing buildings: A critical review on planning energy retrofit strategies for future climate. Renewable and Sustainable Energy Reviews, 199, 114476. https://doi.org/10.1016/j.rser.2024.114476

Natural Resources Canada. Retrieved March 25, 2024, from https://natural-resources.canada.ca/energy-efficiency/buildings/existing-buildings/retrofitting/20707.